Atmos. Chem. Phys. Discuss., 8, 3961–4000, 2008
www.atmos-chem-phys-discuss.net/8/3961/2008/

Atmospheric Chemistry and Physics Discussions

The roles of convection, extratropical mixing, and in-situ freeze-drying in the tropical tropopause layer

W. G. Read[1], M. J. Schwartz[1], A. Lambert[1], H. Su[1], N. J. Livesey[1], W. H. Daffer[1], and C. D. Boone[2]

[1]Jet Propulsion Laboratory, California Institute of Technology, Pasadena, CA, USA
[2]Department of Chemistry, University of Waterloo, Ontario, Canada

Received: 14 December 2007 – Accepted: 4 January 2008 – Published: 26 February 2008

Correspondence to: W. G. Read (bill@mls.jpl.nasa.gov)

Published by Copernicus Publications on behalf of the European Geosciences Union.

Abstract

Mechanisms for transporting and dehydrating air across the tropical tropopause layer (TTL) are investigated with a conceptual two dimensional (2-D) model. The 2-D TTL model combines the Holton and Gettelman cold trap dehydration mechanism (Holton and Gettelman, 2001) with the two column convection model of Folkins and Martin (2005). We investigate 3 possible transport scenarios through the TTL: 1) slow uniform ascent across the level of zero radiative heating without direct convective mixing, 2) convective mixing of H_2O vapor at 100% relative humidity with respect to ice (RHi) with no ice retention, and 3) convective mixing of extremely subsaturated air (convective dehydration) with sufficient ice retention such that total H_2O is 100% RHi. The three mechanisms produce similar seasonal cycles for H_2O that are in good quantitative agreement with the Aura Microwave Limb Sounder (MLS) measurements. We use Aura MLS measurement of CO and Atmospheric Chemistry Experiment-Fourier Transform Spectrometer measurement of HDO to distinguish among the transport mechanisms. Model comparisons with the observations support the view that H_2O is predominantly controlled by the cold trap temperature but the trace species CO and HDO show evidence of extratropical mixing and convective mixing of subsaturated tropospheric air and lofted ice. The model provides some insight into the processes affecting the long term trends observed in stratospheric H_2O.

1 Introduction

Water vapor enters the stratosphere in the tropics (Brewer, 1949; Holton et al., 1995) through convective injection and diabatic ascent. Of particular interest is the long term trend in stratospheric H_2O. A steady increase at twice the rate expected due to oxidation from rising CH_4 persisted for nearly a half century (Rosenlof et al., 2001). After 2000, water vapor showed a sharp decrease (Fueglistaler and Haynes, 2005; Nedoluha et al., 2003; Randel et al., 2006; Rosenlof and Reid, 2008). Dehydration and

transport mechanisms that operate near the tropical tropopause, augmented by CH_4 oxidation are believed to have significant roles in these trends. Much progress has been made recently in our understanding of how air is dehydrated. Models incorporating large scale horizontal transport through cold traps do an excellent job of reproducing the observed seasonal cycle of tropical H_2O entering the stratosphere (Hartmann et al., 2001; Holton and Gettelman, 2001; Jensen et al., 2001; Bonazzola and Haynes, 2004; Fueglistaler et al., 2004; Jensen and Pfister, 2004; Fueglistaler et al., 2005; Fueglistaler and Haynes, 2005; Randel et al., 2006). An alternative hypothesis proposing dehydration of H_2O by convective mixing of extremely subsaturated air (Sherwood and Dessler, 2001, 2003; Danielsen, 1982, 1993) was shown to be inconsistent with the vertical structure of Upper Atmosphere Research Satellite Microwave Limb Sounder (MLS) H_2O between the upper troposphere and the tropopause (Read et al., 2004) and the variability observed in the isotopologues of H_2O (Webster and Heymsfield, 2003). Studies using cloud resolving models show that while convection can inject dry air, condensed ice is not removed quickly enough to produce net dehydration (Grosvenor et al., 2007; Jensen et al., 2007; Smith et al., 2006).

Although a convective signature is not prevalent in H_2O or needed to explain either its annual oscillation (Mote et al., 1996) or its stratospheric entry concentration (e.g., Fueglistaler et al., 2005), observations of other tracers show evidence of convective influence. In addition, clear sky radiative heating calculations indicate that there is a transport barrier 1–2 km below the cold-point tropopause (CPT) in the tropics (Folkins et al., 1999). The transport barrier or level of zero radiative heating (LZH) is where air above rises and air below sinks. The existence of the LZH below the CPT makes the region in between unique, having both tropospheric and stratospheric behaviors and is usually known as the tropical tropopause layer (TTL, Sherwood and Dessler, 2000). Observations of CO_2 (Andrews et al., 1999) and CO (Schoeberl et al., 2006) have seasonal cycles at the tropopause that are present in these molecules in the boundary layer. As explained by Sherwood and Dessler (2003); Folkins et al. (2006b); Schoeberl et al. (2006), convection is needed to transport boundary layer air across the clear-sky

LZH into the TTL.

Observations of the heavy isotopologues of H_2O, HDO and $H_2^{18}O$ show concentrations that are significantly higher than expected from a pure temperature controlled freeze-drying process (Moyer et al., 1996; Johnson et al., 2001a; Kuang et al., 2003). It has been postulated that evaporation of convectively lofted ice (Moyer et al., 1996) provides the additional HDO and $H_2^{18}O$. Evidence of ice lofting and in situ freeze-drying was observed from aircraft (Webster and Heymsfield, 2003) in subtropical convection. Several studies employing different mechanisms have successfully reproduced observations of HDO (Dessler and Sherwood, 2003; Gettelman et al., 2004; Schmidt et al., 2005; Dessler et al., 2007); however, none of these models incorporate both in situ freeze-drying and convective mixing of dry air and lofted ice as suggested by cloud resolving models. Here we present a conceptual model that incorporates both in situ freeze drying and convective mixing. We run the model using 3 different representations of convection and transport across the TTL. The representation where convection detrains ice, air having low relative humidity with respect to ice (RHi), and tropospheric CO successfully reproduces the tropical zonal mean observations of H_2O, CO, and HDO.

2 CCT-TTL Model Description

The convection/cold trap TTL (CCT-TTL) model used here is based upon the two dimensional (2-D) conceptual model developed by Holton and Gettelman (2001, herein after referred to as HG01). The model includes a parameterization for convective mixing (Folkins and Martin, 2005) and computes vapor and ice mixing ratios of H_2O, HDO and $H_2^{18}O$, and the mixing ratio of CO. The model is a 2-D representation (longitude by height) of the TTL. The vertical domain of the model covers 14–19 km and the horizontal domain is 18 000 km. The Aura MLS v1.5 temperature drives the model. The Aura MLS v1.5 temperature has three measurements between 14 and 19 km (147, 100, and 68 hPa). A warm bias of 1.5 K is removed (Schwartz et al., 2008). The tropical (12° S–

12° N) MLS temperature measurements are averaged in 14 equally spaced longitude bins. The daily temperature profile at the 147 and 68 hPa levels is the tropical average. The 100 hPa daily temperature which defines the CPT temperature in the CCT-TTL model comes from the longitude bin having the warmest average. The model's daily background temperature profile (T_0 in Eq. 1 of HG01) is linearly interpolated vertically and temporally from the Aura MLS temperature profile previously described.

The CPT height in the model is specified to be at 100 hPa and 16.5 km without seasonal variation. Although the true CPT height varies with season, this difference is not resolved in the v1.5 Aura MLS temperature field. As in HG01, we superimpose on T_0, a cold trap represented by a 2500 km×1 km Gaussian function. The temperature in the cold trap is taken from the longitude bin having the coldest Aura MLS 100 hPa temperature again interpolated linearly in time to the model time step.

The CCT-TTL model includes no parameterization for gravity wave perturbations (Pfister et al., 2001; Jensen and Pfister, 2004; Potter and Holton, 1995). Since gravity wave features are present in the Aura MLS temperatures (Wu et al., 2006), the CCT-TTL model does not necessarily need an additional parameterization for them; however, some gravity waves remain unresolved by Aura MLS. Neglecting these waves should cause the model to overestimate H_2O entering the stratosphere. Quantifying this error is difficult because the magnitude of unresolved gravity waves is unknown and are compensated by random noise in the Aura MLS temperature measurement. A rough estimate of this effect is derived from applying a 7 day high-pass filter to the minimum Aura MLS CPT temperature time series. The resulting time series visually looks like random noise having a standard deviation of 0.5 K. The sum of amplitudes of all waves having a period less than 7 days in the Jensen and Pfister (2004) model is 1 K. Therefore the impact of gravity waves may be underestimated by 0.5 K. Vapor and ice are partitioned according to HG01 and Folkins et al. (2006b)

$$\begin{aligned}\frac{D[X]_v}{Dt} &= -\frac{[X]_v - [X]_v^{\mathrm{ex}}}{\tau_\alpha} + K\frac{\partial^2[X]_v}{\partial z^2} + \frac{[X]_i}{\tau_E} - \frac{[X]_v - [X]_s}{\tau_c} \\ &\quad - \frac{[X]_v - [X]_v^{\mathrm{conv}}}{\tau_d} + P - L[X]_v, \\ \frac{D[X]_i}{Dt} &= -\frac{[X]_i - [X]_i^{\mathrm{ex}}}{\tau_\alpha} + K\frac{\partial^2[X]_i}{\partial z^2} - \frac{[X]_i}{\tau_E} + \frac{[X]_v - [X]_s}{\tau_c} \\ &\quad - \frac{[X]_i - [X]_i^{\mathrm{conv}}}{\tau_d}. \end{aligned} \quad (1)$$

The right hand terms in Eq. (1) going from 1st to 7th describe extratropical mixing, vertical diffusion, evaporation, condensation, convective mixing, chemical production and loss. The subscripts v, i, and s, on concentration $[X]$ refer to vapor, condensed phase, and vapor over condensed phase. Superscript conv and ex refer to convective and extratropical concentrations respectively.

The extratropical mixing rate profile, τ_α (30 days at 14 km and 580 days at 19 km) is that used in HG01. The extratropical supply of H_2O, CO, HDO, and $H_2^{18}O$, are based on observations. The extratropical $[H_2O]_v^{\mathrm{ex}}$ is 5.5, 4.2, and 3.8 parts per million volume (ppmv) at 147(≈14 km), 100(=16.5 km), and 68 hPa(≈19 km) based on the extratropical average of Aura MLS v1.5 measurements. We use linear interpolation to compute concentrations on the model vertical grid. Extratropical CO from Aura MLS is 70, 49, 26 parts per billion volume (ppbv) at the previously mentioned heights. The isotopologues are expressed as δD or δ^{18}O (‰)=1000[R×(HDO or $H_2^{18}O$) /H_2O-1) where R is (HDO or $H_2^{18}O$)/H_2O in Vienna standard mean ocean water. For δD we use the average multiyear Atmospheric Chemistry Experiment-Fourier Transform Spectrometer (ACE-FTS, Bernath et al., 2005) 30° N/S–40° N/S measurement of −596‰ from 150–100 hPa. For δ^{18}O we use −128‰ from Johnson et al. (2001b). The extratropical $[X]_i^{\mathrm{ex}}$ for all species is zero.

The vertical diffusion constant K is 0.03 m^2/s (Andrews et al., 1999; Mote et al., 1998).

The convective detrainment (mixing) rate, d, is diagnosed from the prescribed large scale upwelling and extratropical mass flux divergence according to the two column model (TCM, Folkins and Martin, 2005). The upwelling and its seasonal cycle are derived from TCM results published in Folkins et al. (2006b, their Fig. 1,with the mass flux profiles shifted vertically to align their LZH with that used in the CCT-TTL model). The LZH is 15.5 km in the CCT-TTL model. The seasonal cycle for the upwelling is phased such that its maximum occurs on 14 February. The TCM calculations show that the maximum vertical velocity occurs ∼1 km above the LZH with a slight decline above.

Downwelling of air associated with radiative cooling from subvisible cirrus lying above deep convective anvil clouds (Hartmann et al., 2001) is parameterized according to HG01. The downward velocity is proportional to the ice mixing ratio in the cold trap as prescribed by HG01.

Figure 1 shows the clear-sky vertical velocity with its annual oscillation. The prescribed velocity is consistent with other estimates (Mote et al., 1998; Randel et al., 2002; Andrews et al., 1999; Rosenlof, 1995). According to the TCM, the rate at which air detrains from the cloudy column is balanced by the radiative mass flux divergence of the clear sky column and the mass flux divergence to higher latitudes. Mathematically, $1/\tau_d = \partial\omega/\partial p + 1/\tau_\alpha$, where ω is the radiative heating vertical mass flux which is proportional to the vertical velocity. It is worth noting that the convective detrainment rate profile is not a free parameter in both models. The seasonal variability of the computed convective detrainment rate profile is given in Fig. 1. Convective detrainment rates were diagnosed from CO and O_3 profiles taken from the February 1996 Stratospheric Tracers of Atmospheric Transport campaign (Dessler, 2002). The convective detrainment rate profile in Fig. 1 is shorter (faster) but within the uncertainty of that diagnosed from O_3 and CO gradients up to the CPT. The convective supply terms, $[X]_v^{\text{conv}}$ and $[X]_i^{\text{conv}}$ whose values are most uncertain are discussed later.

The vapor/ice equations are solved for the time evolution of $[X]_v$ and $[X]_i$ using a semi-Lagrangian algorithm described in Staniforth and Côté (1991). The horizontal

domain utilizes periodic boundary conditions. The horizontal velocity is 10 m/s (HG01). Water vapor and CO in the lowest altitude grid point for all longitudes is the v1.5 Aura MLS 147 hPa tropical zonal mean measurement interpolated to the model time. The heavy isotopologues use δD=−650‰ (from tropical ACE-FTS measurements at 150 hPa) and δ^{18}O=−154‰ (Webster and Heymsfield, 2003) for HDO and $H_2^{18}O$ respectively. The model is run from August 2003 to February 2007, the month Aura MLS v1.5 data ended. The first year is used to spin-up the model and uses Aura MLS temperature data from August 2004 to July 2005 for the 2003/2004 period.

2.1 H_2O modeling

The evaporation and condensation rates, τ_E=1 day, and τ_c=1 h, are those used in HG01. Condensation, the 4th term in Eq. (1), vanishes except when $[H_2O]_v \geq 100\%$ RHi and $[H_2O]_i > 0$ or $[H_2O]_v \geq 160\%$ RHi and $[H_2O]_i = 0$ (Jensen et al., 2001; Koop et al., 1998). Ice sediments at a velocity proportional to its effective radius according to a relation given in Boehm et al. (1999). The effective radius of the ice particles is parameterized according to their ice water content (IWC, McFarquhar and Heymsfield, 1997). The sedimentation rates are typically ∼7 mm/s for ∼6.5 μm radius particles.

The production P, and loss L, terms are highly parameterized in this model. For H_2O we use 1.8×10^{-8} ppmv/s and 0 for the production and loss respectively. The production term due to CH_4 oxidation is estimated from the vertical gradient of H_2O.

2.2 CO modeling

Carbon monoxide is useful for testing the convective parameterization in the model (Folkins et al., 2006a). As has been noted before, when RHi≥100%, temperature control dominates convective mixing making it difficult to observe any evidence of convective influence on H_2O. This is readily seen in Eq. (1). The condensation rate in supersaturated air is much faster (1 h) than the convective mixing rate (≥20 days) in the TTL. The non-condensible tropospheric tracer CO on the other hand, is especially

valuable for detecting convective activity in the TTL. In the CCT-TTL model, CO is represented by the time tendency of the vapor equation and all terms involving condensed phases vanish. The 5th term representing convection stands out. Carbon monoxide is destroyed by OH in the lower stratosphere, producing a vertical gradient. The production and loss rates for CO use the profiles in Folkins et al. (2006a). As shown in Randel et al. (2006), Schoeberl et al. (2007), and Folkins et al. (2006b), an annual cycle in CO is produced above the tropopause as a consequence of modulating the vertical gradient in CO by the annual oscillation in the vertical upwelling. Therefore CO is a good diagnostic of both convection and the large scale upwelling.

2.3 HDO and $H_2^{18}O$ modeling

The heavy water isotopologues condense more efficiently than H_2O as temperature is lowered. As a result, δD becomes progressively smaller than its surface ratio as rising air is freeze-dried. Therefore δD provides insight into the temperature of the air parcel's most recent condensation event or if convection is mixing deuterium (or ^{18}O) enriched ice.

The CCT-TTL model partitions HDO and $H_2^{18}O$ according to Eq. (1). The Rayleigh fractionation is applied to the $[X]_v^{conv}$ and $[X]_s$ quantities. When the model decides that a cloud is formed, the frost point temperature of $[H_2O]_v$ is calculated prior to evaluating Eq. (1). Next $[HDO]_s$ is computed from $[HDO]_v$ by integrating the Rayleigh fractionation function from the frost point temperature to the environmental temperature. If $[H_2O]_v/[H_2O]_s>1$ after applying Eq. (1), there will be a kinetic isotope effect which inhibits preferential condensation of HDO. The same procedure is applied to $H_2^{18}O$. The fractionation factors and theory are from Johnson et al. (2001a) and include the kinetic isotope effect (Jouzel and Merlivat, 1984) with updated diffusivity ratios (Cappa et al., 2003). Production of HDO and $H_2^{18}O$ from CH_3D and CH_4 oxidation is that for H_2O scaled by $\delta D=-70‰$ and $\delta^{18}O=-23‰$, respectively (Schmidt et al., 2005). We assume no chemical loss.

2.4 Role of convection

The CCT-TTL model is used to investigate three convective transport scenarios summarized in Table 1. The first scenario "slow ascent" (SA) limits convection's influence to providing only large scale upwelling without any direct mixing. The CCT-TTL model has a uniform vertical velocity of 0.23 mm/s (with a seasonal amplitude of 0.8 mm/s) throughout the TTL without a LZH and convective mixing. This is the original HG01 model and emulates the convective mechanism in trajectory based models (Gettelman et al., 2002; Jensen and Pfister, 2004; Fueglistaler et al., 2005) where the large scale vertical motion allows some trajectories to cross the clear sky LZH. The second and third scenarios incorporate convective mixing according to the vertical velocity and convective mixing rate profiles in Fig. 1.

The convective mixing schemes explore the sensitivity of H_2O, HDO, and $H_2^{18}O$, to different mechanisms for control of $[H_2O]_v^{conv}$ and $[H_2O]_i^{conv}$, summarized in Table 1. $[H_2O]_v^{conv}$ and $[H_2O]_i^{conv}$ are free parameters in this model and are not well constrained by observations. Temperature provides some constraint on $[H_2O]_v^{conv}$ as it is unlikely to exceed ~100% RHi for the environmental temperature. Ice however is much more uncertain. A factor complicating matters is that convectively lofted ice represents a spectrum of particle sizes and fall speeds. Observations and numerical simulations using cloud resolving models show ice concentrations of ~1000 part per million volume (ppmv) in the TTL (Webster and Heymsfield, 2003; Jensen et al., 2007). The majority of this ice is unlikely to mix in the TTL because it will sediment too quickly. Therefore $[H_2O]_i^{conv}$ is probably best represented by the ice concentrations in the small particle radius tail ($r<20\,\mu$m) of the convectively lofted ice particle size distribution. According to the microphysical model in Jensen et al. (2007), small particle ice concentrations have $[H_2O]_i^{conv}<6$ ppmv. Although the $[H_2O]_v^{conv}$ and $[H_2O]_i^{conv}$ in Table 1 are uncertain, they represent plausible values.

The Convection-No Ice (C-NOICE) case activates the 5th term in Eq. (1) where 100% RHi computed at a modified environmental temperature T′ is mixed into the

TTL. The modified environmental temperature is the environmental temperature below the CPT and above, T′ is the mean of the environmental temperature and the moist adiabatic temperature extrapolated upward from the CPT (Pfister and Jensen, 2007). The modified environmental temperature continues to cool above the CPT because the moist adiabat cools more rapidly than the environmental temperature warms, consistent with outgoing longwave radiation (OLR) measurements that are sometimes less than the CPT temperature. In this scheme all convective ice is removed. Following Keith (2000) we assume deep convection lofts air from the cloud base into the TTL without significant mixing. Accordingly, convectively supplied $[HDO]_v^{conv}$ (δD∼−900‰ at the CPT) and $[H_2^{18}O]_v^{conv}$(δ^{18}O∼−200‰ at the CPT) follow Rayleigh fractionation.

The third case, convection following Sherwood and Dessler (2001, hereafter referred as SD01) with Ice retention (CSD01-ICE) revisits their convective dehydration model where 100% RHi air at a convective temperature, T^{conv}, following the moist adiabat from the level of neutral buoyancy (set at 160 hPa) is mixed into the environmental air. Cloud resolving models lend support to the likelihood that temperature inside overshooting convective turrets is much colder than the environment (Grosvenor et al., 2007; Smith et al., 2006; Jensen et al., 2007). The CSD01-ICE scheme differs from SD01 by convectively supplying enough ice to inhibit dehydration. Convective dehydration is not supported by observations or cloud resolving model calculations that show enough ice evaporates after convection collapses to prevent significant dehydration. For a consistent comparison to the C-NOICE test we mix enough ice such that the total H_2O is the same as that in the C-NOICE test. This is equivalent to increasing the ice retention parameter from 4 to 10 in the SD01 model at the CPT. As with C-NOICE, $[HDO]_v^{conv}$ and $[H_2^{18}O]_v^{conv}$ follow the Rayleigh fractionation for 100% RHi at T^{conv}. Because $T^{conv} < T'$, the H_2O isotopologues mix vapor that is even more depleted than that used by C-NOICE; however, ice carries enriched D and ^{18}O such that δD and $\delta^{18}O$ in total water are −550‰ and −80‰ respectively. The isotopic ratios for the total H_2O isotopologues are tunable parameters in this model and we choose values that represent Rayleigh fractionation of vapor up to the level of neutral buoyancy for tropical convection.

3 Data

3.1 Aura MLS measurements

Aura MLS measures millimeter–sub millimeter wavelength thermal emission from the Earth's atmospheric limb (Waters et al., 2006). The Aura MLS fields of view point in the direction of orbital motion and vertically scan the limb in the orbit plane. Aura MLS produces almost 3500 atmospheric profiles over 14 orbits between 82° S to 82° N each day.

This study compares the model output to Aura MLS v1.5 and v2.2 H_2O and v1.5 CO. As was noted earlier, the CCT-TTL model is driven by Aura MLS v1.5 tropical temperature. The precision (uncertainty left over after removing the 1.5 K warm bias) and vertical resolution of the v1.5 temperature measurement are 1 K and 6 km (Livesey, 2005; Schwartz et al., 2008). Extratropical averages of Aura MLS v1.5 H_2O and CO are used for the extratropical mixing concentrations. The tropical average of 147 hPa Aura MLS v1.5 H_2O and CO are input into the bottom of the model, and the tropical 147 hPa Aura MLS v1.5 CO is the CO convective input. The accuracy for v2.2 H_2O is 7–12%, with a 3–3.5 km vertical resolution and a single profile precision of 15% (Read et al., 2007, v1.5 H_2O is similar). The version 2.2 H_2O vertical retrieval grid has twice as many levels as v1.5 in the troposphere and lower stratosphere. The accuracy, vertical resolution and single profile precision for v2.2 CO is 30%±20 ppbv, 4 km, and 20 ppbv (Livesey et al., 2008, v1.5 CO is similar). All Aura MLS data sets were appropriately screened according to rules given in Livesey (2007) and Livesey (2005).

3.2 ACE-FTS

The HDO measurements are provided by ACE-FTS on the Canadian SCISAT-1 mission (Bernath et al., 2005). ACE-FTS is a high resolution (0.02 cm^{-1}) infrared Fourier transform spectrometer that measures solar occultation spectra between 2.2 and 13.3 μm (750–4400 cm^{-1}). Vertical profiles are retrieved for up to 15 sunrises and

15 sunsets per day whose latitudes vary over an annual cycle from 85° S to 85° N with an emphasis on the polar regions during winter and spring. The current processing version for the ACE-FTS is version 2.2 (Boone et al., 2005). We use here an official update to the processing called "version 2.2 HDO update" (Nassar et al., 2007), which corrects errors in HDO results found in the original version 2.2 dataset. The ACE-FTS HDO retrievals employ 18 microwindows (spectral intervals of width 0.3–0.5 cm^{-1}) in the wavenumber range 1400–1500 cm^{-1} and 6 microwindows in the range 2610–2675 cm^{-1}.

The altitude range for the HDO retrievals extends from 5 to 38 km. Data for the other isotopologues are not yet released. The vertical resolution and precision of the ACE-FTS HDO are 3–4 km and 20–40‰. The ACE-FTS HDO is not yet validated but results presented in this paper agree well with earlier tropical HDO measurements from Atmospheric Trace MOlecule Spectroscopy (ATMOS, Kuang et al., 2003; Gunson et al., 1996) and Aircraft Laser Infrared Absorption Spectrometer (ALIAS, Webster and Heymsfield, 2003). The isotopologue comparisons concentrate on the 2005–2007 time frame where ACE-FTS and Aura MLS v1.5 measurements overlap. Applying the recommended quality screening to the ACE-FTS data produces 260 profiles between 12° S and 12° N.

4 Results

4.1 H_2O

Figure 2 compares H_2O time series for the 3 CCT-TTL model runs (SA, C-NOICE, and CSD01-ICE) to v1.5 Aura MLS at 147, 100, and 68 hPa. The Aura MLS H_2O measurements are daily zonal means between 12° S–12° N. Figure 3 shows the same comparison for the partially complete Aura MLS v2.2 H_2O on 147, 121, 100, 83, and 68 hPa. The model runs have been convolved with the Aura MLS averaging kernel (Rodgers, 1990) and the forward model smoothing function (Read et al., 2007, 2006). The obser-

vations clearly show that the maximum amplitude in the H_2O annual oscillation occurs at 100 hPa in v1.5 and 83 hPa in v2.2. The phase of the annual oscillation shifts with altitude reflecting the transit time of air from the CPT where the annual oscillation is imprinted. This feature is often referred to as a tape recorder (Mote et al., 1996). There is little to no annual oscillation at 147 and 121 hPa in the Aura MLS H_2O. This closely follows the tropical temperature data that shows an annual oscillation <1 K at 14 km becoming 6 K at the CPT (Randel et al., 2002). Noteworthy is 20% dryness of the v2.2 147 hPa H_2O relative to v1.5. This reflects a change in how the two different Aura MLS versions vertically resolve the data which is particularly evident at 147 and 100 hPa in the tropics (Read et al., 2007). The lower Aura MLS v2.2 147 hPa H_2O measurements indicate a sharper change in the vertical gradient in H_2O below the CPT which is consistent with a transport barrier at 14 km (Folkins et al., 1999).

Despite the different transport and convective mixing parameterizations, the model runs show mostly good agreement with each other and the Aura MLS measurements. This result emphasizes the dominance of cold trap CPT temperature control—common to all parameterizations—in regulating the entry of H_2O into the stratosphere. This is expected because condensation is the fastest of all processes in Eq. (1). All that matters is that H_2O transported into the cold trap is greater than 100% RHi (or 160% RHi to initiate condensation). The SA run vertically advects ∼10 ppmv H_2O from 14 km which is greater than the SMR of the cold trap temperature. The C-NOICE convection directly injects 100% RHi air throughout the TTL (at a rate decreasing with altitude) including regions outside of the cold trap. Moisture injected above the LZH that is vertically and horizontally advected through the cold trap is greater than its SMR. The CSD01-ICE introduces two competing processes, one that injects air ≪100% RHi and another that injects ice some of which can reevaporate.

The largest difference among the convective transport schemes occurs during the Boreal summertime at the CPT. This is caused by an inability of the SA and CSD01-ICE convective parameterizations to maintain 100% RHi in the cold trap during the warm phase. This is caused by dehydration from extratropical mixing below the CPT during

the warm phase. The similar behavior of the SA and CSD01-ICE transport schemes suggests that convection in CSD01-ICE neither hydrates nor dehydrates the TTL for Table 1 H_2O amounts. The C-NOICE convection scheme supplies enough moisture to maintain the model cold trap at 100% RHi all year. H_2O from the C-NOICE has a larger annual oscillation.

The better agreement between Aura MLS and the SA or CSD01-ICE results does not necessarily justify rejecting the C-NOICE mechanism. Of concern is the oft-cited issue of using Eularian grid box temperature averages in place of averages of minimum temperature encountered along trajectories (e.g., Fueglistaler et al., 2004). The cold trap temperature field in the CCT-TTL model has a 7.7 K annual oscillation. The Lagrangian cold point based on trajectory analysis using European Center for Medium Range Weather Forecasts 40-year Reanalysis (ERA-40) temperature fields from 1992–2001 has a smaller 4.3 K annual oscillation (Fueglistaler et al., 2004). Due to the nonlinear response of the SMR to temperature, H_2O during the warm season is exaggerated. If the CCT-TTL model followed the trajectory analysis temperature, then all three transport scenarios considered here will maintain 100% RHi in the cold trap all year and produce very similar results and H_2O could not be used to distinguish amongst them.

There is additional evidence that temperature driven freeze-drying occurs all year. Subvisible cirrus near the CPT is present all year (Wang et al., 1996). Fluctuations in model H_2O seen in the C-NOICE run which are caused by similar fluctuations in the Aura MLS temperature field during the Boreal summers qualitatively follow those in the Aura MLS H_2O lending some evidence that the Boreal summer is also under cold trap temperature control and that the Boreal summer MLS longitude bin average having the minimum cold point temperature is too warm. The fluctuations which have a periodicity of 1–2 months when present are probably CPT temperature anomalies associated with the Madden Julian Oscillation (Madden and Julian, 1994; Wong and Dessler, 2007).

There is no evidence that convection dehydrates the TTL because dehydrating convection would produce a drier Boreal summer than observed and reduces the ampli-

tude of the annual oscillation in H_2O. This happens when $[H_2O]_i^{conv}$ is made smaller (not shown). Increasing $[H_2O]_i^{conv}$ in CSD01-ICE above that in Table 1 causes this convection scheme to have a moistening effect in the TTL similar to that for C-NOICE.

4.2 CO

Figure 4 shows a time-height view of Aura MLS v1.5 CO from August 2004 to March 2007. Aura MLS observations of CO show a semiannual oscillation propagating up to the CPT and an annual oscillation at the top of the TTL. These features are generally understood to be the combined effects of convective mixing of boundary layer air polluted with CO from biomass burning and the annual oscillation of the tropical upwelling acting on the vertical gradient of CO (Schoeberl et al., 2006; Randel et al., 2007; Folkins et al., 2006b; Schoeberl et al., 2007).

The second panel shows results from the SA run vertically smoothed by the Aura MLS averaging kernel and forward model smoothing function. Because it lacks convective mixing, it fails to produce a semiannual oscillation, producing only an annual oscillation through most of the model domain caused by the annual oscillation in the upwelling. Although the Aura MLS CO measurement containing the semiannual cycle is sourced into the bottom of the model, the upwelling is slow compared to the extratropical mixing and the semiannual cycle is washed out. Turning-off extratropical mixing produces a semiannual CO tape recorder (not shown) originating at 147 hPa that is inconsistent with observations.

The third panel shows the CSD01-ICE (C-NOICE is similar) run, again vertically smoothed by the Aura MLS averaging kernel. Adding convective mixing accurately reproduces all the major observed features. The only shortcoming is that the amplitude of the observed features are underestimated. Performing the same model run without extratropical mixing (not shown) causes the annual oscillation to dominate the CO variability throughout the TTL replicating a calculation shown in Folkins et al. (2006b) (Fig. 3). This occurs for two reasons: 1) removing extratropical mixing steepens the CO vertical gradient (from chemical decay), and 2) the convective mixing rate is reduced

(the convective detrainment rate loses a contribution from the extratropical mixing) and reduces to zero just below the CPT. The CO measurements are sensitive to extratropical mixing, chemical loss, upwelling and convective mixing. Nevertheless, these comparisons clearly show that convection is mixing air into the TTL up to the CPT.

The observed CO features are also reproduced with the Goddard Modeling Initiative (GMI) Chemical Transport Model (CTM, Schoeberl et al., 2006). The GMI-CTM is driven by GEOS-4 meteorology. Like our model, the GMI-CTM underestimates the amplitude of the semiannual oscillation in CO. The semiannual oscillation in CO doesn't propagate to as high an altitude as in the CCT-TTL model or in Aura MLS CO. This feature is consistent with the behaviors of the Zhang and McFarlane (1995, GEOS-4/GMI-CTM) and TCM (CCT-TTL) convection schemes (Folkins et al., 2006a).

4.3 HDO

Figure 5 shows a comparison between an ACE-FTS 2-year (2005/2006) tropical average δD profile and the model runs. The ACE-FTS δD profile shows a weak, slightly positive gradient in the TTL. This is broadly consistent with ATMOS (Kuang et al., 2003) δD. Quantitatively the values are in excellent agreement(~ -650‰, same as ATMOS). Also shown are the individual measurement points. Like ATMOS, most of the ACE-FTS δD measurements fall within $\sim$50‰ of the mean. Overlaid is the 2 year average δD from the 3 CCT-TTL model runs. Each run is shown as a pair of lines (total of 6 lines). The solid lines are model runs that include extratropical mixing and the dashed lines have no extratropical mixing.

The SA run without extratropical mixing falls between the two Rayleigh distillation curves that represent the seasonal extremes. This is expected because only temperature controlled freeze-drying occurs. The kinetic isotope effect is negligible in these model runs because H_2O rapidly relaxes to 100% RHi upon condensation. It is worth mentioning however, observations show that the base of the TTL is significantly enriched in HDO relative to the 1-D Rayleigh distillation from the surface. This is evidence of reevaporation of HDO enriched ice detrained from tropical deep convection (Keith,

2000). The solid line showing excellent agreement with observations includes extratropical mixing. The good agreement achieved by including extratropical mixing results from a process that relaxes the TTL to extratropical observations and should not be interpreted as support for lack of evidence for direct convective mixing. Stratospheric mixing in the Gettelman and Webster (2005) isotopologue model is treated similarly and may have helped that model achieve good results without direct convective mixing.

The C-NOICE run, shows the poorest agreement with observations. Without extratropical mixing, δD follows Rayleigh distillation from the surface and is much too depleted. Even with extratropical mixing, δD is still too depleted. This implies that in the tropics, convection does not remove all its ice and detrians only vapor, consistent with the Keith (2000) investigation who arrived at the same conclusion. Of course it is possible that convection supplies ice in addition to vapor. Therefore we performed another test run where $[H_2O]_i^{conv}=[H_2O]_v^{conv}=[H_2O]_s(T')$ again with and without extratropical mixing. Without extratropical mixing, δD has a minimum of -720‰ which is less than observed. Extratropical mixing increases the minimum δD to -670‰ which is in better agreement with observations but H_2O above the CPT is 0.5–1 ppmv higher than the Aura MLS observations all year. Therefore it appears difficult to simultaneously achieve good agreement with H_2O and δD with convection mixing 100% RHi vapor in the TTL.

The CSD01-ICE runs show best agreement with ACE-FTS observations with and without extratropical mixing. Perhaps most importantly, it produces a nearly constant δD ratio in the TTL in the absence of extratropical mixing. This point was strongly emphasized as favorable support for the overshooting convection dehydration model (Dessler and Sherwood, 2003). The self consistency of the two runs eliminates the need to invoke a separate mechanism to explain the extratropical δD ratio. The result in Fig. 5 is insensitive to the amount of ice retained. Doubling the ice retention has no effect on δD except to improve agreement with ACE-FTS between 121–147 hPa. Mixing more ice causes convection to have a moistening effect similar to the C-NOICE

scheme where the cold trap freeze-dries air entering the stratosphere all year. The insensitivity of δD to the amount of retained ice precludes its quantification. Also note that the CSD01-ICE (and C-NOICE) model run unlike SA does not depend on the δD prescribed for the lower model boundary because air sinks at this level.

The reason why CSD01-ICE is so effective at enriching the air with HDO is its ability to mix and reevaporate HDO enriched ice even in saturated environmental air. A convection scheme detraining 100% RHi, inhibits ice evaporation and hence the δD remains close to that of the convective vapor. In the SD01 representation, convection dessicates the air which allows more HDO enriched ice to evaporate. Ice evaporates even if the environmental air is initially saturated. This is the fundamental difference between the recent Dessler et al. (2007, DHF07 hereinafter) modification to the Fueglistaler et al. (2005) model and the earlier Dessler and Sherwood (2003) model and the CSD01-ICE configuration described here. The DHF07 model uses a mixing scheme based on temporally relaxing the environment to 100% RHi using HDO enriched vapor. As trajectories encounter saturated regions, convection does nothing. Therefore convection has its greatest impact on low relative humidity air. However, the average relative humidity of the TTL and upper troposphere is generally quite high ~50–75% RHi making convective enrichment less effective. This is why DHF07 needs to use a much higher δD ratio (−100‰) in convectively detrained vapor to achieve the same effect as −565‰ did in their earlier model.

Figure 6 shows a time series of the δD measured by ACE-FTS and computed by the CSD01-ICE model run between 100 and 80 hPa. We show the time and value of all the ACE-FTS measurements to reveal the seasonality and spread of measurements. A smoothed running mean for the ACE-FTS measurements is overlaid. A 2-D snapshot of the CCT-TTL model is saved for each month. The model data plotted represent only 24 discrete times, each separated by 1 month. The longitudinal spread is shown in shaded grey with its running mean overlaid. Because we only save a small sample among many time steps, the variation is certainly underestimated but is sufficient to convey the basic behavior. The model shows a weak annual oscillation that is smaller

than the spread of measurements seen in the ACE-FTS observations. Perhaps not surprisingly, the model produces minimum δD during the cold dry phase of the annual oscillation in CPT temperatures. The running mean of the ACE-FTS data also show a weak seasonal dependence but with opposite phasing.

The model also shows an annual oscillation in the spread of δD ratios whose maximum occurs during the cold phase of the CPT temperature annual cycle. The cold phase has a stronger longitudinal gradient in δD because convective supply of HDO enriched ice is re-depleted by in situ Rayleigh distillation in the cold trap. During the warm phase of the CPT temperature oscillation, in situ Rayleigh distillation in the cold trap is weak and convective ice detrainment and extratropical mixing both of which have constant δD ratios dominate. ACE-FTS doesn't show a strong annual oscillation in the spread of HDO throughout the year. This is further evidence that the cold trap temperature is dehydrating air throughout the year and that the measurement, and/or longitude bin averaging of the Boreal summer Aura MLS temperatures used by the CCT-TTL model are too warm.

4.4 $H_2^{18}O$

Figure 7 shows model calculations for δ^{18}O. Unfortunately there are no global data sets yet available for comparisons. However, we have shown an average of clear sky/TTL-screened measurements from ALIAS during the Cirrus Regional Study of Tropical Anvils and Cirrus Layers–Florida Area Cirrus Experiment campaign (Webster and Heymsfield, 2003; Gettelman and Webster, 2005). The model results are interesting because the relative behavior of δD to δ^{18}O is useful to detect persistent supersaturation. Currently, there is much speculation regarding how supersaturated the tropopause is (Jensen et al., 2005). In situ aircraft measurements of H_2O in the TTL support high persistent supersaturation whereas satellite and balloon frost point hygrometers show less. The difference is ~30% near the tropopause between Aura MLS and balloon frost point versus a suite of in situ hygrometers flown on the WB57 aircraft (Read et al., 2007).

It is known that the distillation of isotopologues in supersaturated air affects $\delta^{18}O$ more strongly than δD and therefore $\delta^{18}O$ relatively speaking will show less depletion and greater departures from Rayleigh fractionation. It has been argued that the weak dependence of observed $\delta^{18}O$ relative to δD as a function of H_2O in the uppermost troposphere was evidence of significant supersaturation occurring in thin cirrus clouds (Gettelman and Webster, 2005). This is not a robust conclusion however because our modeling study shows that the CSD01-ICE scheme also produces similar behavior given the limited amount of available data without supersaturation. It is worth noting that published results from models by Gettelman and Webster (2005) and Schmidt et al. (2005) like the CCT-TTL model produce less depleted $\delta^{18}O$ ratios than observed by ALIAS but are within its large uncertainty.

5 Conclusions

We have described a 2-D conceptual (CCT-TTL) model that includes a cold trap, extratropical mixing, and convection. The CCT-TTL model is used to study how in situ freeze-drying, extratropical mixing and convection affect the concentration of H_2O, HDO, $H_2^{18}O$, and CO entering the tropical stratosphere.

We summarize our findings as follows. Based on model comparisons with Aura MLS H_2O, at least 9 months out of the year, H_2O entering the stratosphere is set by the cold trap temperature. The processes that occur during the Boreal summer are less certain. The values and/or bin averaging of the v1.5 Aura MLS temperatures suggest that the cold trap during the Boreal summer is warm enough to let other processes dominate such as extratropical mixing; however, temporal wave structure in the Aura MLS cold trap temperature is also present in Aura MLS H_2O, supporting temperature control for these months. Since we believe the wave structure in the Aura MLS temperature is more robust than the accuracy associated with the longitude bin averaging as well as the measurement of temperature itself, we conclude that H_2O is under cold trap temperature control all year. Spatial variability seen in ACE-FTS δD throughout the

year also supports year-long CPT temperature control. All year cold trap temperature control is supported by more detailed models such as Fueglistaler et al. (2005). Since extratropical mixing dehydrates the TTL during the Boreal summer, convection must hydrate to maintain H_2O at the CPT at its SMR. The Aura MLS CO measurement clearly provides evidence for convective mixing in the TTL up to at least the CPT. The heavy water isotopologues support convective mixing of both subsaturated air and ice. Because the δD (or $\delta^{18}O$) profile is very insensitive to the amount of ice retained, they provide no constraint on how much ice is detrained.

These studies may shed some light on the stratospheric H_2O trend puzzle (Rosenlof et al., 2001). A number of ideas have been advanced which include widening of the tropical upwelling belt (Zhou et al., 2001; Seidel et al., 2007), relative changes in the seasonal circulation (Rosenlof and Reid, 2008), and microphysical changes in convection associated with increased aerosol loading from biomass burning (Sherwood, 2002). Because of successes in modeling stratospheric entry H_2O during the last ~15 years with a temperature control model it has also been suggested that the historical data may be suspect as its implied entry H_2O is too dry to be explained by CPT temperature control (Fueglistaler and Haynes, 2005). We urge some caution in accepting this view because H_2O entering the stratosphere may not have always been under CPT temperature control.

The decade long increase in stratospheric H_2O could be evidence of strengthening convective influence putting the TTL under cold trap temperature control throughout the year. Here we assume that convection has a moistening effect between the LZH and the CPT. A simple scenario has the declining CPT temperature trend associated with increased upwelling (Randel et al., 2006) which in turn leads to increased convective mixing in the TTL (Fig. 1, Folkins et al., 2006a). It is possible that decades ago, weaker upwelling would have weakened convective mixing above the LZH, allowing extratropical mixing to maintain a subsaturated cold trap during a significant portion of the year. The annual average H_2O entering the stratosphere would be closer to Boreal winter-time values. As upwelling increases, convective moistening in the TTL increases

the percentage of the year that the TTL is under cold trap temperature control. This causes an increase in H_2O because the warmer temperature SMRs fold into the annual average. Once the TTL is under cold trap temperature control all year, the long term trend in the CPT temperature takes effect causing the decline observed in contemporary H_2O measurements (Randel et al., 2006). Figure 8 shows schematically how this might work. Microphysical processes as suggested by Sherwood (2002), supported by Grosvenor et al. (2007), when coupled to the CSD01-ICE scheme may explain the extreme aridity implied by the pre-1980 data by providing an explanation that could cause convection to transition over time from a dehydrating to a hydrating source in the TTL.

Acknowledgements. The authors thank S. Sherwood, A. Dessler, and K. Rosenlof for helpful comments and suggestions. The research described here done at the Jet Propulsion Laboratory, California Institute of Technology, was under contract with the National Aeronautics and Space Administration. We thank the Canadian Space Agency (CSA) for funding the ACE mission and supplying the HDO data.

References

Andrews, A. E., Boering, K. A., Daube, B. C., Wofsy, S. C., Hintsa, E. J., Weinstock, E. M., and Bui, T. P.: Empirical age spectra for the lower tropical stratosphere from in-situ observations of CO_2: Implications for stratospheric transport, J. Geophys. Res., 104, 26 581–26 595, 1999. 3963, 3966, 3967

Bernath, P. F., McElroy, C., Abrams, M., Boone, C., Butler, M., Camy-Peyret, C., Carleer, M., Clerbaux, C., Coheur, P., Colin, R., DeCola, P., DeMazire, M., Drummond, J., Dufour, D., Evans, W., Fast, H., Fussen, D., Gilbert, K., Jennings, D., Llewellyn, E., Lowe, R., Mahieu, E., McConnell, J., McHugh, M., McLeod, S., Michaud, R., Midwinter, C., Nassar, R., Nichitiu, F., Nowlan, C., Rinsland, C., Rochon, Y., Rowlands, N., Semeniuk, K., Simon, P., Skelton, R., Sloan, J., Soucy, M.-A., Strong, K., Tremblay, P., Turnbull, D., Walker, K., Walkty, I., Wardle, D., Wehrle, V., Zander, R., and Zou, J.: Atmospheric Chemistry Experiment (ACE): Mission Overview, Geophys. Res. Lett., 32, L15S01, doi:10.1029/2005GL022386, 2005. 3966, 3972

Boehm, M. T., Verlinde, J., and Ackerman, T. P.: On the Maintenance of High Tropical Cirrus, J. Geophys. Res., 104, 24 423–24 433, 1999. 3968

Bonazzola, M. and Haynes, P. H.: A trajectory-based study of the tropical tropopause region, J. Geophys. Res., 109, D20112, doi10:1029/2003JD000511, 2004. 3963

Boone, C. D., Nassar, R., Walker, K., Rochon, Y., McLeod, S., Rinsland, C., and Bernath, P.: Retrievals for the Atmospheric Chemistry Experiment Fourier-transform spectrometer, Appl. Optics, 44, 7218–7231, 2005. 3973

Brewer, A. W.: Evidence for a world circulation provided by the measurements of helium and water vapour distribution in the stratosphere, Q. J. R. Meteorol. Soc., 75, 351–363, 1949. 3962

Cappa, C. D., Hendricks, M. B., DePaolo, D. J., and Cohen, R. C.: Isotopic Fractionation of Water during Evaporation, J. Geophys. Res., 108, 4525, doi:10.1029/2003JD003597, 2003. 3969

Danielsen, E. F.: A dehydration mechanism for the stratosphere, Geophys. Res. Lett., 9, 605–608, 1982. 3963

Danielsen, E. F.: In situ evidence of rapid, vertical irreversible transport of lower tropospheric air into the lower stratosphere by convective cloud turrets and by large-scale upwelling in tropical cyclones, J. Geophys. Res., 98, 8665–8681, 1993. 3963

Dessler, A. E.: The Effect of Deep, Tropical Convection on the Tropical Tropopause Layer, J. Geophys. Res., 107, 4033, doi:10.1029/2001JD000511, 2002. 3967

Dessler, A. E. and Sherwood, S. C.: A model of HDO in the tropical tropopause layer, Atmos. Chem. Phys., 3, 4489–4501, 2003, http://www.atmos-chem-phys.net/3/4489/2003/. 3964, 3978, 3979

Dessler, A. E., Hanisco, T. F., and Füglistaler, S. A.: The effects of convective ice lofting on H_2O and HDO in the TTL and tropical lower stratosphere, J. Geophys. Res., 112, D18309, doi:10.1029/2007JD008609, 2007. 3964, 3979

Folkins, I. and Martin, R. V.: The Vertical Structure of Tropical Convection and its Impact on the Budgets of Water Vapor and Ozone, J. Atmos. Sci., 62, 1560–1573, 2005. 3962, 3964, 3967

Folkins, I., Loewenstein, M., Podolske, J., Oltmans, S. J., and Proffit, M.: A barrier to vertical mixing at 14 km in the tropics: Evidence from ozonesondes and aircraft measurements, J. Geophys. Res., 104, D18, 22 095–22 102, 1999. 3963, 3974

Folkins, I., Bernath, P., Boone, C., Donner, L. J., Lesins, G., Martin, R. V., Sinnhuber, B.-M., and Walker, K.: Testing convective parameterizations with tropical measurements of HNO_3, CO, H_2O, O_3: Implications for the water vapor budget, J. Geophys. Res., 111, D23304, doi:10.1029/2006JD007325, 2006a. 3968, 3969, 3977, 3982

Folkins, I., Bernath, P., Boone, C., Lesins, G., Thompson, A. M., Walker, K., and White, J. C.: Seasonal cycles of O_3, CO, and convective outflow at the tropical tropopause, Geophys. Res. Lett., 33, 16, L16802, doi:10.1029/2006GL026602, 2006b. 3963, 3965, 3967, 3969, 3976

Fueglistaler, S. and Haynes, P. H.: Control of interannual and longer-term variability of stratospheric water vapor, J. Geophys. Res., 110, D24108, doi:10.1029/2005JD006019, 2005. 3962, 3963, 3982

Fueglistaler, S., Wernli, H., and Peter, T.: Tropical troposphere-to-stratosphere transport inferred from trajectory calculations, J. Geophys. Res., 109, D03108, doi:10.1029/2003JD004069, 2004. 3963, 3975

Fueglistaler, S., Bonazzola, M., Haynes, P. H., and Peter, T.: Stratospheric water vapor predicted from the Lagrangian temperature histroy of air entering the stratosphere in the tropics, J. Geophys. Res., 110, D08107, doi:10.1029/2004JD005516, 2005. 3963, 3970, 3979, 3982

Gettelman, A., Randel, W. J., Wu, F., and Massie, S. T.: Transport of water vapor in the tropical tropopause layer, Geophys. Res. Lett., 29, 1, 1009, doi:10.1029/2001GL013818, 2002. 3970

Gettelman, A. E. and Webster, C. R.: Simulations of water isotope abundances in the upper troposphere and lower stratosphere and implications for stratosphere troposphere exchange, J. Geophys. Res., 110, D17301, doi:10.1029/2004JD004812, 2005. 3978, 3980, 3981

Gettelman, A. E., Weinstock, E. M., Fetzer, E. J., Irion, F. W., Eldering, A., Richard, E. C., Rosenlof, K. H., Thompson, T. L., Pittman, J. V., Webster, C. R., and Herman, R. L.: Validation of satellite data in the upper troposphere and lower stratosphere with in-situ aircraft instruments, Geophys. Res. Lett., 31, L22107, doi:10.1029/2004GL020730, 2004. 3964

Grosvenor, D. P., Choularton, T. W., Coe, H., and Held, G.: A study of the effect of overshooting deep convection on the water content of the TTL and lower stratosphere from Cloud Resolving Model simulations, Atmos. Chem. Phys., 7, 4977–5002, 2007, http://www.atmos-chem-phys.net/7/4977/2007/. 3963, 3971, 3983

Gunson, M. R., Abbas, M. M., Abrams, M. C., Allen, M., Brown, L. R., Brown, T. L., Chang, A. Y., Goldman, A., Irion, F. W., Lowes, L. L., Mahieu, E., Manney, G. L., Michelson, H. A., Newchurch, M. J., Rinsland, C. P., Salawitch, R. J., Stiller, G. P., Toon, G. C., Yung, Y. L., and Zander, R.: The Atmospheric Trace Molecule Spectroscopy (ATMOS) experiment: Deployment on the ATLAS Space Shuttle missions, Geophys. Res. Lett., 23, 2333–2336, 1996. 3973

Hartmann, D. L., Holton, J. R., and Fu, Q.: The heat balance of the tropical tropopause, cirrus,

and stratospheric dehydration, Geophys. Res. Lett., 28, 1969–1972, 2001. 3963, 3967

Holton, J. R. and Gettelman, A.: Horizontal transport and the dehydration of the stratosphere, Geophys. Res. Lett., 28, 2799–2802, 2001. 3962, 3963, 3964

Holton, J. R., Haynes, P. H., McIntyre, M. E., Douglass, A. R., Rood, R. B., and Pfister, L.: Stratosphere-troposphere exchange, Rev. Geophys., 33, 403–439, 1995. 3962

Jensen, E. J. and Pfister, L.: Transport and freeze-drying in the tropical tropopause layer, J. Geophys. Res., 109, D2, D02207, doi:10.1029/2003JD004022, 2004. 3963, 3965, 3970

Jensen, E. J., Pfister, L., Ackerman, A. S., and Tabazedeh, A.: A conceptual model of the dehydration of air due to freeze-drying by optically thin, laminar cirrus rising slowly across the tropical tropopause, J. Geophys. Res., 106, D15, 17 237–17 252, 2001. 3963, 3968

Jensen, E. J., Smith, J. B., Pfister, L., Pittman, J. V., Weinstock, E. M., Sayres, D. S., Herman, R. L., Troy, R. F., Rosenlof, K., Thompson, T. L., A, M, F., Hudson, P. K., Cziczo, D. J., Heymsfield, A. J., Schmitt, C., and Wilson, J. C.: Ice supersaturations exceeding 100% at the cold tropical tropopause: implications for cirrus formation and dehydration, Atmos. Chem. Phys., 5, 851–862, 2005, http://www.atmos-chem-phys.net/5/851/2005/. 3980

Jensen, E. J., Ackerman, A. S., and Smith, J. A.: Can overshooting convection dehydrate the tropical tropopause layer?, J. Geophys. Res., 112, D11209, doi:10.1029/2006JD007943, 2007. 3963, 3970, 3971

Johnson, D. G., Jucks, K. W., Traub, W. A., and Chance, K. V.: Isotopic composition of stratospheric water vapor: Implications for transport, J. Geophys. Res., 106, 12 219—12 226, 2001a. 3964, 3969

Johnson, D. G., Jucks, K. W., Traub, W. A., and Chance, K. V.: Isotopic composition of stratospheric water vapor: Measurements and Photochemistry, J. Geophys. Res., 106, 12 211—12 217, 2001b. 3966

Jouzel, J. and Merlivat, L.: Deuterium and Oxygen 18 in Precipitation: Modeling of the Isotopic Effects During Snow Formation, J. Geophys. Res., 99, 11 749–11 757, 1984. 3969

Keith, D. W.: Stratosphere-troposphere exchange: Inferences from the isotopic composition of water vapor, J. Geophys. Res., 105, 15 167–15 173, 2000. 3971, 3977, 3978

Koop, T., Ng, H. P., Molina, L. T., and Molina, M. J.: A New Optical Technique to Study Aerosol Phase Transitions: The Nucleation of Ice from H_2SO_4 Aerosols, J. Chem. Phys., 102, 8924–8931, 1998. 3968

Kuang, Z., Toon, G. C., Wennberg, P. O., and Yung, Y. L.: Measured HDO/H_2O ratios across the tropical tropopause, Geophys. Res. Lett., 30, 1372, doi:10.1029/2003GL017023, 2003.

3964, 3973, 3977
Lanzante, J. R., Klein, S. A., and Seidel, D. J.: Temporal Homogenization of Monthly Radiosonde Temperature Data. Part II: Trends, Sensitivities, and MSU Comparison, J. Climate, 16, 241–262, 2003. 4000
Livesey, N. J.: Data Quality Document for the EOS MLS version 1.5 Level 2 Dataset, Tech. Rep., Jet Propulsion Laboratory, 35–40, 45–52, 105–109, 2005. 3972
Livesey, N. J.: Data Quality Document for the EOS MLS version 2.2 Level 2 Dataset, Tech. Rep., Jet Propulsion Laboratory, 39–44, 2007. 3972
Livesey, N. J., Froidevaux, L., Read, W. G., Lambert, A., Cofield, R. E., Fuller, R. A., Jarnot, R. F., Jiang, J. H., Jiang, Y. B., Knosp, B. W., Santee, M. L., Schwartz, M. J., Snyder, W. V., Stek, P. C., Wagner, P. A., Waters, J. W., Pumphrey, H. C., Avery, M., Browell, E. V., Christiensen, L. E., Loewenstein, M., Lopez, J. D., Sachse, G. W., and Webster, C. R.: Validation EOS Microwave Limb Sounder O_3 and CO observations in the upper troposphere/lower stratosphere, J. Geophys. Res., 113, doi:10.1029/2007JD008805, in press, 2008. 3972
Madden, R. A. and Julian, P. R.: Observations of the 40–50 Day Tropical Oscillation—A Review, Mon. Weather Rev., 122, 814–837, 1994. 3975
McFarquhar, G. M. and Heymsfield, A. J.: Parameterization of Tropical Cirrus Ice Crystal Size Distributions and Implications for Radiative Transfer: Results from CEPEX, J. Atmos. Sci., 54, 2187–2200, 1997. 3968
Mote, P. W., Rosenlof, K. H., McIntyre, M. E., Carr, E. S., Gille, J. C., Holton, J. R., Kinnersley, J. S., Pumphrey, H. C., III, J. M. R., and Waters, J. W.: An atmospheric tape recorder: The imprint of tropical tropopause temperatures on stratospheric water vapor, J. Geophys. Res., 101, 3989–4006, 1996. 3963, 3974
Mote, P. W., Dunkerton, T. J., McIntyre, M. E., Ray, E. A., Haynes, P. H., and III, J. M. R.: Vertical Velocity, Vertical Diffusion, and Dilution by Midlatitude Air in the Tropical Lower Stratosphere, J. Geophys. Res., 103, 8651–8666, 1998. 3966, 3967
Moyer, E. J., Irion, F. W., Yung, Y. L., and Gunson, M. R.: ATMOS stratospheric water and implications for tropospheric-stratospheric transport, Geophys. Res. Lett., 23, 2385–2388, 1996. 3964
Nassar, R., Bernath, P. F., Boone, C. D., Gettelman, A., McLeod, S. D., and Rinsland, C. P.: Variability in HDO/H_2O abundance ratios in the tropical tropopause layer, J. Geophys. Res., 112, D21305, doi:10.1029/2007JD008417, 2007. 3973

Nedoluha, G. E., Bevilacqua, R. M., Gomez, R. M., Siskind, D. E., Hicks, B. C., Russell, III, J. M., and Connor, B. J.: An evaluation of trends in middle atmospheric water vapor as measured by HALOE, WVMS, and POAM, J. Geophys. Res., 108, D13, 4391, doi:10.1029/2002JD003332, 2003. 3962
Pfister, L. and Jensen, E.: Convective Influence Calculations for CR-AVE and TC4, in: 14th Conference on Middle Atmosphere, American Meteorological Society, Portland Oregon, P3.12, 2007. 3971
Pfister, L., Selkirk, H. B., Jensen, E. J., Schoeberl, M. R., Toon, O. B., Browell, E. V., Grant, W. B., Gary, B., Mahoney, M. J., Bui, T. V., and Hintsa, E.: Aircraft observations of thin cirrus clouds near the tropical tropopause, J. Geophys. Res., 106, D9, 9765–9786, 2001. 3965
Potter, B. E. and Holton, J. R.: The Role of Mesoscale Convection in the Dehydration of the Lower Tropical Stratosphere, J. Atmos. Sci., 52, 1034–1050, 1995. 3965
Randel, W. J., Garcia, R. R., and Wu, F.: Time-Dependent Upwelling in the Tropical Lower Stratosphere Estimated from the Zonal-Mean Momentum Budget, J. Atmos. Sci., 59, 2141–2152, 2002. 3967, 3974
Randel, W. J., Wu, F., Vömel, H., Nedoluha, G. E., and Forster, P.: Decreases in Stratospheric Water Vapor after 2001: Links to Changes in the Tropical Tropopause and the Brewer-Dobson Circulation, J. Geophys. Res., 111, D12312, doi:10.1029/2005JD006744, 2006. 3962, 3963, 3969, 3982, 3983
Randel, W. J., Park, M., Wu, F., and Livesey, N.: A Large Annual Cycle in Ozone above the Tropical Tropopause Linked to the Brewer-Dobson Circulation, J. Atmos. Sci., 64, 4479–4488, 2007. 3976
Read, W. G., Wu, D. L., Waters, J. W., and Pumphrey, H. C.: Dehydration in the tropical tropopause layer: Implications from the UARS Microwave Limb Sounder, J. Geophys. Res., 109, D06110, doi:10.1029/2003JD004056, 2004. 3963
Read, W. G., Shippony, Z., and Snyder, W. V.: The Clear-Sky Unpolarized Forward Model for the EOS Aura Microwave Limb Sounder (MLS), IEEE T. Geosci. Remote, The EOS Aura Mission, 44, 1367–1379, 2006. 3973
Read, W. G., Bacmeister, J., Cofield, R. E., Cuddy, D. T., Daffer, W. H., Drouin, B. J., Fetzer, E., Froidevaux, L., Fuller, R., Herman, R., Jarnot, R. F., Jiang, J. H., Jiang, Y. B., Kelly, K., Knosp, B. W., Kovalenko, L. J., Lambert, A., Lay, R., Livesey, N. J., Liu, H.-C., Loo, M., Manney, G. L., Miller, D., Mills, B. J., Pickett, H. M., Pumphrey, H. C., Rosenlof, K. H., Sabounchi, X., Santee, M. L., Schwartz, M. J., Snyder, W. V., Stek, P. C., Su, H., Takacs, L. L.,

Thurstans, R. P., Vömel, H., Wagner, P. A., Waters, J. W., Weinstock, E. M., and Wu, D. L.: EOS Aura Microwave Limb Sounder Upper Tropospheric and Lower Stratospheric Humidity Validation, J. Geophys. Res., 112, D24S35, doi:10.1029/2007JD008752, 2007. 3972, 3973, 3974, 3980, 3994, 3995, 3996

Rodgers, C. D.: Characterization and error analysis of profiles retrieved from remote sounding measurements, J. Geophys. Res., 95, D5, 5587–5595, 1990. 3973

Rosenlof, K. H.: Seasonal cycle of the residual mean meridional circulation in the stratosphere, J. Geophys. Res., 100, D3, 5173–5191, 1995. 3967

Rosenlof, K. H. and Reid, G. C.: Trends in the temperature and water vapor content of the tropical lower stratosphere: The Sea-Surface Connection, J. Geophys. Res., 113, doi:10.1029/2007JD009109, in press, 2008. 3962, 3982

Rosenlof, K. H., Oltmans, S. J., Kley, D., III, J. M. R., Chiou, E.-W., Chu, W. P., Johnson, D. G., Kelly, K. K., Michelsen, H. A., Nedoluha, G. E., Remsberg, E. E., Toon, G. C., and McCormick, M. P.: Stratospheric water vapor increases over the past half-century, Geophys. Res. Lett., 28, 1195–1198, 2001. 3962, 3982

Schmidt, G. A., Hoffmann, G., Shindell, D. T., and Hu, Y.: Modeling Atmospheric Stable Water Isotopes and the Potential for Constraining Cloud Processes and Stratosphere-Troposphere Water Exchange, J. Geophys. Res., 110, D21314, doi:10.1029/2005JD005790, 2005. 3964, 3969, 3981

Schoeberl, M. R., Duncan, B. N., Douglass, A. R., Waters, J., Livesey, N., Read, W., and Filipiak, M.: The Carbon Monoxide Tape Recorder, Geophys. Res. Lett., 33, L12811, doi:10.1029/2006GL026178, 2006. 3963, 3976, 3977

Schoeberl, M. R., Douglass, A. R., Newman, P. A., Lait, L. R., Lary, D., Waters, J., Livesey, N., Froidevaux, L., Lambert, A., Read, W., Filipiak, M., and Pumphrey, H.: QBO and Annual Cycle Variations in the Tropical Lower Stratosphere Trace Gases from HALOE and Aura MLS Observations, J. Geophys. Res., 112, doi:10.1029/2007JD008678, 2007. 3969, 3976

Schwartz, M. J., Lambert, Manney, G., Read, W., Livesey, N., Froidevaux, L., Ao, C., Bernath, P., Boone, C., Cofield, R., Daffer, W., Drouin, B., Fetzer, E., Fuller, R., Jarnot, R., Jiang, J., Jiang, Y., Knosp, B., Kruger, K., Li, J.-L., Mlynczak, M., Pawson, S., III, J. R., Santee, M., Snyder, W., Stek, P., Thurstans, R., Tompkins, A., Wagner, P., Walker, K., Waters, J., and Wu, D.: Validation of the Aura Microwave Limb Sounder Temperature and Geopotential Height Measurements, J. Geophys. Res., 113, doi:10.1029/2007JD008783, in press, 2008. 3964, 3972

Seidel, D. J., Fu, Q., Randel, W. J., and Reichler, T. J.: Widening of the Tropical Belt in a Changing Climate, Nature Geoscience, doi:10.1038/ngeo.2007.38, http://www.nature.com/ngeo/journal/vaop/ncurrent/index.html, 2007. 3982

Sherwood, S. C.: A microphysical connection among biomass burning, cumulus clouds, and stratospheric moisture, Science, 295, 1272–1275, 2002. 3982, 3983

Sherwood, S. C. and Dessler, A. E.: On the control of stratospheric humidity, Geophys. Res. Lett., 27, 2513–2516, 2000. 3963

Sherwood, S. C. and Dessler, A. E.: A model for transport across the tropical tropopause, J. Atmos. Sci., 58, 765–779, 2001. 3963, 3971

Sherwood, S. C. and Dessler, A. E.: Convective mixing near the tropical tropopause: insights from seasonal variations, J. Atmos. Sci., 60, 2674–2685, 2003. 3963

Smith, J. A., Ackerman, A. S., Jensen, E. J., and Toon, O. B.: Role of Deep Convection in Establishing the Isotopic Composition of Water Vapor in the Tropical Transition Layer, Geophys. Res. Lett., 33, L06812, doi:10.1029/2005GL024078, 2006. 3963, 3971

Staniforth, A. and Côté, J.: Semi-Langrangian Integration Schemes for Atmospheric Models–A Review, Mon. Weather Rev., 119, 2206–2223, 1991. 3967

Wang, P.-H., Minnis, P., McCormick, M. P., Kent, G. S., and Skeens, K. M.: A 6-year climatology of cloud occurrence frequency from Stratospheric Aerosol and Gas Experiment II observations (1985–1990), J. Geophys. Res., 101, 29 407–29 429, 1996. 3975

Waters, J. W., Froidevaux, L., Harwood, R. S., Jarnot, R. F., Pickett, H. M., Read, W. G., Siegel, P. H., Cofield, R. E., Filipiak, M. J., Flower, D. A., Holden, J. R., Lau, G. K., Livesey, N. J., Manney, G. L., Pumphrey, H. C., Santee, M. L., Wu, D. L., Cuddy, D. T., Lay, R. R., Lou, M. S., Perun, V. S., Schwartz, M. J., Stek, P. C., Thurstans, R. P., Boyles, M. A., Chandra, K. M., Chavez, M. C., Chen, G.-S., Chudasama, B. V., Dodge, R., Fuller, R. A., Girard, M. A., Jiang, J. H., Jiang, Y., Knosp, B. W., LaBelle, R. C., Lam, J. C., Lee, K. A., Miller, D., Oswald, J. E., Patel, N. C., Pukala, D. M., Quintero, O., Scaff, D. M., Snyder, W. V., Tope, M. C., Wagner, P. A., and Walch, M. J.: The Earth Observing System Microwave Limb Sounder (EOS MLS) on the Aura satellite, IEEE T. Geosci. Remote., The EOS Aura Mission, 44, 1075–1092, 2006. 3972

Webster, C. R. and Heymsfield, A. J.: Water isotope ratios D/H, $^{18}O/^{16}O$, $^{17}O/^{16}O$ in and out of clouds reveal dehydration pathways and the origin of cirrus, Science, 302, 1742–1745, 2003. 3963, 3964, 3968, 3970, 3973, 3980

Wong, S. and Dessler, A. E.: Regulation of H_2O and CO in the Tropical Tropopause Layer by

the Madden-Julian Oscillation, J. Geophys. Res., 112, D14305, doi:10.1029/2006JD007940, 2007. 3975

Wu, D. L., Preusse, P., Eckermann, S., Jiang, J., de la Torre Juarez, M., Coy, L., and Wang, D.: Remote Sounding of Atmospheric Gravity Waves with Satellite Limb and Nadir Techniques, Adv. Space Res., 37, 2269–2277, 2006. 3965

Zhang, G. J. and McFarlane, N. A.: Sensitivity of climate simulations to the parameterization of cumulus convection in the Canadian Climate Centre General Circulation Model, Atmos. Ocean., 33, 407–446, 1995. 3977

Zhou, X.-L., Geller, M. A., and Zhang, M.: Cooling trend of the tropical cold point tropopause temperatures and its implications, J. Geophys. Res., 106, D2, 1511–1522, 2001. 3982

Table 1. CCT-TTL Model Test Runs

Convection Scheme	$1/\tau_d$	T^{conv}	$[H_2O]_v^{conv}$	$[H_2O]_i^{conv}$
Slow Ascent (SA)	0.0	NA	NA	NA
Convection no ice (C-NOICE)	Fig. 1	T'[a]	$[H_2O]_s(T')$	0.0
Convection with ice (CSD01-ICE)	Fig. 1	$T_{lnb}\left(p/p_{lnb}\right)^{2/7}$	$[H_2O]_s(T^{conv})$	$[H_2O]_s(T')$–$[H_2O]_s(T^{conv})$

a T' is the environmental temperature except above the CPT where a modified scheme described in the text is used.

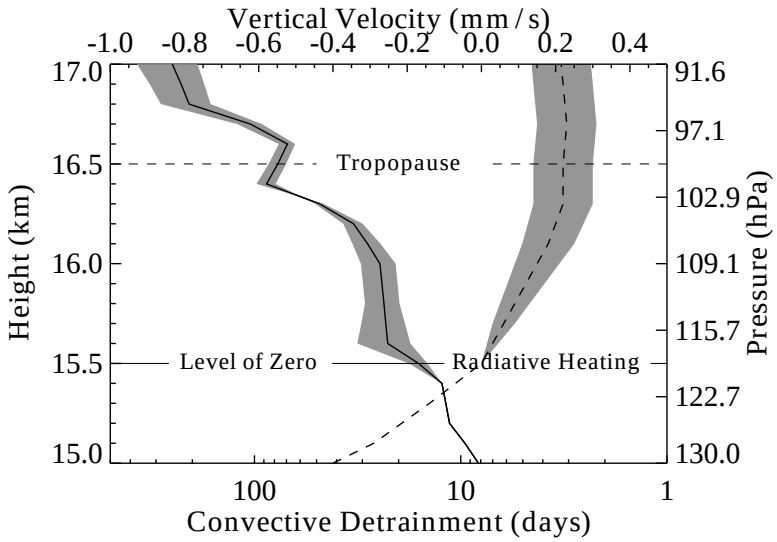

Fig. 1. Vertical velocities, dashed line, and convective mixing rates, solid line, used in the CCT-TTL model. The annual variations are shown by the shaded region about the mean profile. The Boreal summer shows slower upwelling velocities and longer detrainment rates.

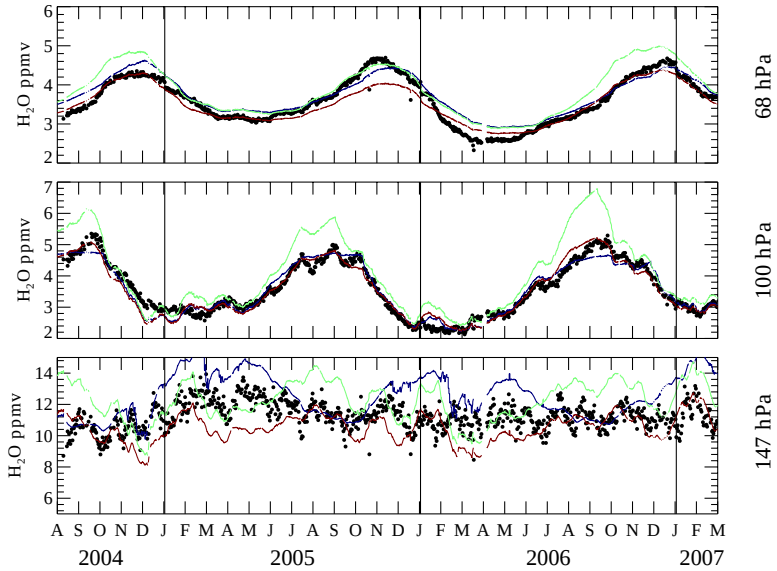

Fig. 2. (black points) H_2O time series at 147, 100, and 68 hPa, for Aura MLS v1.5 , CCT-TTL model runs, (blue) SA, (green) C-NOICE, and (red) CSD01-ICE. The Aura MLS measurements are daily zonal means between 12° S–12° N. The model runs are smoothed by the Aura MLS forward model smoothing function and v1.5 averaging kernel (Read et al., 2007).

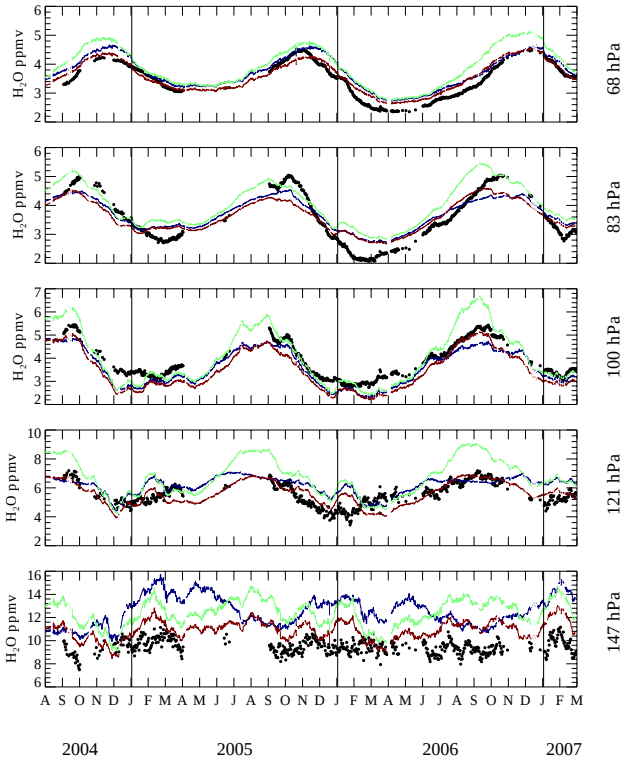

Fig. 3. Same as Fig. 2 except it shows v2.21 Aura MLS H_2O and the model runs are smoothed by the Aura MLS forward model smoothing function and v2.2 averaging kernel (Read et al., 2007).

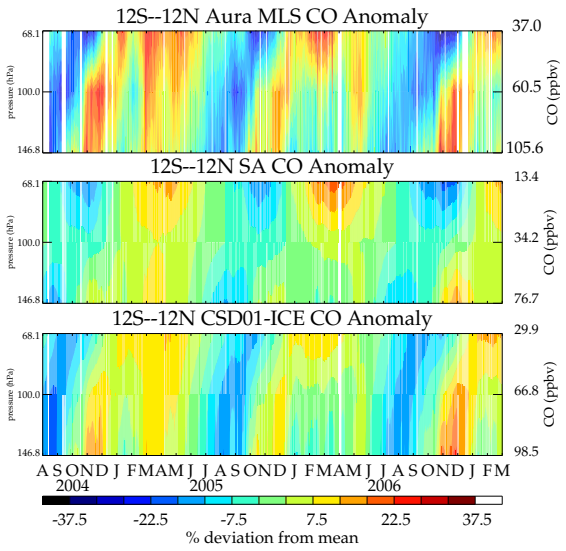

Fig. 4. The top panel shows a time height cross section of Aura MLS v1.5 CO anomaly (percent deviation from the mean) between 12° S and 12° N. The middle panel shows the same from the CCT-TTL SA model run. The bottom panel shows the same for the CCT-TTL CSD01-ICE model run. The model runs have been smoothed by the Aura MLS forward model smoothing function and v1.5 averaging kernel (Read et al., 2007) .

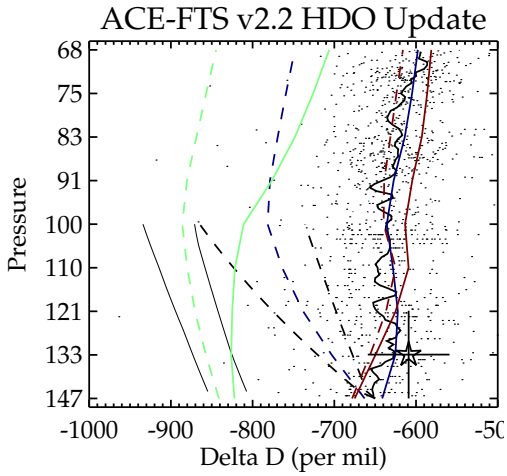

Fig. 5. The black points are ACE FTS measurements of δD between 12° S to 12° N for 2005 and 2006. The mean of the ACE-FTS δD is overlaid (black line). The CCT-TTL model runs for the same time period are (blue) SA, (green) C-NOICE, and (red) CSD01-ICE. The CCT-TTL model runs including tropical mixing are shown as solid lines and without extratropical mixing as dashed lines. The star is an average of TTL measurements made during CRYSTAL-FACE by ALIAS with the vertical bar representing the altitude coverage of the average and the horizontal bar representing accuracy. The thin solid black lines are Rayleigh distillation curves representing the seasonal extremes in temperature from the surface. The thick dashed black lines are Rayleigh distillation curves representing the seasonal extremes beginning at the prescribed δD for the lower TTL boundary.

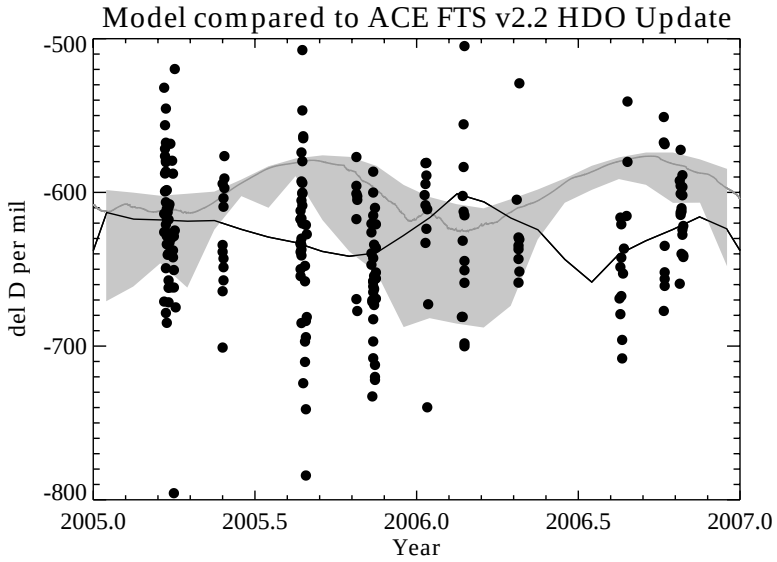

Fig. 6. ACE-FTS δD measurements between 12° S and 12° N between 100 and 80 hPa (solid circles) shown as a function of time. The black solid line is a temporally smoothed mean of the ACE-FTS data. The grey shading represents the longitudinal variation of δD from the CSD01-ICE run. Dark grey is the mean of the CSD01-ICE δD.

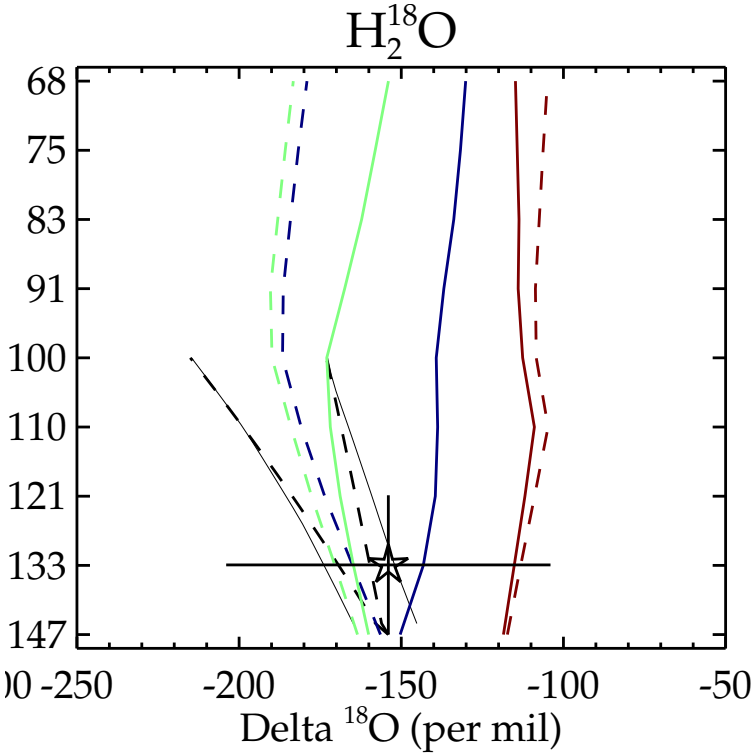

Fig. 7. Same as Fig. 5 but for δ^{18}O.

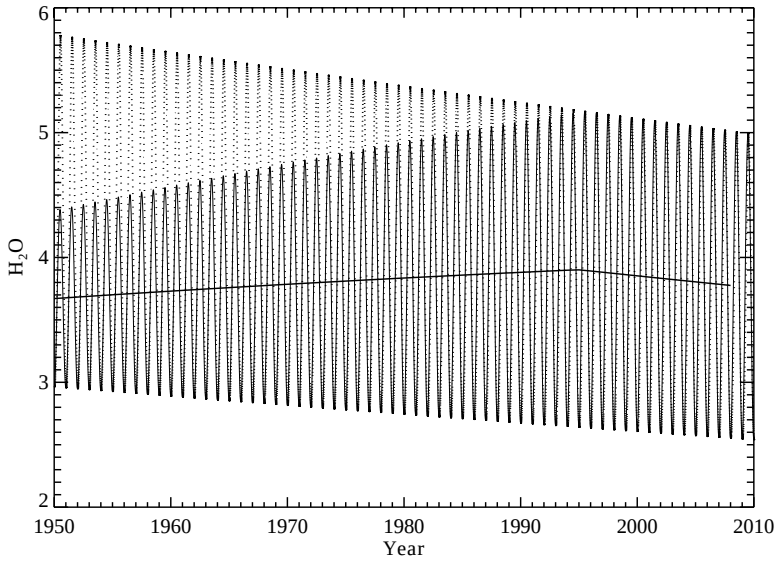

Fig. 8. A schematic representation of how H_2O can show the observed trend as described in the text. The dots are the SMR under cold trap temperature control assuming −0.15 K/decade tropopause temperature trend (Lanzante et al., 2003). The thin line is H_2O under increasing convective influence assumed here to reduce the time the tropics is subsaturated by 1% per year. The thick line is a hypothetical entry H_2O trend.